Carrier-induced modulation of radiation by a gated graphene

M.V. Strikha and F.T. Vasko*
Institute of Semiconductor Physics, NAS of Ukraine, Pr. Nauky 41, Kyiv, 03028, Ukraine
(Dated: September 20, 2011)

The modulation of the transmitted (reflected) radiation due to change of interband transitions under variation of carriers concentration by the gate voltage is studied theoretically. The calculations were performed for strongly doped graphene on high-κ (Al_2O_3, HfO_2, AlN, and ZrO_2) or SiO_2 substrates under normal propagation of radiation. We have obtained the modulation depth above 10% depending on wavelength, gate voltage (i.e. carriers concentration), and parameters of substrate. The graphene - dielectric substrate - doped Si (as gate) structures can be used as an effective electrooptical modulator of near-IR and mid-IR radiation for the cases of high-κ and SiO_2 substrates, respectively.

PACS numbers: 78.67.Wj, 42.79.Hp

I. INTRODUCTION

The essential feature of graphene's optical properties is its substantial interaction with radiation in the wide spectral region, from far-IR up to UV, due to effective interband transitions (see reviews [1]). The enhancement of this responce due to interference permits one to make the graphene on dielectric substrate visible [2]. The other example of the exceptional optical properties is the graphene-based saturable absorber for ultrafast lasers in the telecommunication spectral region [3]. Besides this, the carriers contribution modifies essentially the graphene response due to the Pauli blocking effect, when absorption is supressed at $\hbar\omega/2 < \varepsilon_F$, where ω is the frequency of radiation, ε_F is the Fermy energy, see experimental data and discussion in Refs. 4 and 5. Recently, modulation [6] and polarization [7] of IR radiation were observed in the graphene structure integrated with an optical waveguide. The efficiency of modulation can also be enhanced for the case of normal propagation of radiation by the interference effect under an appropriate thickness of substrate, see Figs. 1a and 1b. As a result, an improvement of modulation for transmission and reflection coefficients of the graphene - substrate - gate structure by a gate voltage takes place in contrast to the case of graphene placed on a semi-infinete insulator. [8] In this paper, we perform the calculation of the optical characteristics of such a structure, and we discuss the conditions for realisation of the graphene-based modulator in the near- and mid-IR spectral region.

At low temperatures, or high doping levels, the threshold frequency for the jump of absorption is determined by the condition $\hbar\omega_{th} = 2\varepsilon_F \propto \sqrt{n}$, where concentration n depends linearly on gate voltage, V_g, and is inverse to substrate thickness, d, so that $n \propto V_g/d \equiv E_\perp$. The dependences of the threshold wavelength λ_{th} on homogeneous field $E_\perp$ are presented in Fig. 1c for a number of substrates. One can see that the modulation of near-IR radiation (1.55 μm) is possible at $E_\perp$ <3 MV/cm for the high-κ substrates (Al_2O_3, HfO_2, AlN, and ZrO_2 are examined below), and for SiO_2 substrate the applied field should be twice stonger. The modulation of mid-IR radiation (10.6 μm) can be realised in lower fieids, $E_\perp$ < 1 MV/cm. For the modulation of radiation in the visible spectral range, a field $E_\perp$ comparable with the breakdown field for the substrate under consideration is needed. The modulation depth can be estimated through the amplitude of the absorbtion jump on the threshold, equal to 2.3%. For the 5 layer graphene the modulation efficiency can exceed 10%, taking into account that the interference on substrate influences this value. The absorption edge spreads with the increase of temperature (see the real part of dynamic conductivity σ_ω presented in Fig. 1d), and the modulation efficiency decreases. At room temperature the effective modulation for near-IR radiation only is possible, while the modulation of mid-IR radiation needs cooling to temperatures about 77 K. The efficiency of modulation obtained is comparable to results both in bulk semiconductors and in heterostructures, see Refs. 9 and 10, respectively.

The analysis performed below is organized as follows. In Sect. II we describe the carrier-induced modulation of the response of graphene and evaluate the transmission and reflection coefficients. The efficiency of modulation versus applied field and thickness of substrate is analyzed in Sect. III. Discussion and concluding remarks are given in the last section.

II. BASIC EQUATIONS

The response of a doped graphene sheet on probe radiation is described by the two-dimensional dynamic conductivity σ_ω. In the colisionless approximation, when ω exceeds any relaxation rate, the real and imaginary parts of σ_ω are given by the expressions:

$$\mathrm{Re}\sigma_\omega \simeq \frac{e^2}{4\hbar}(1 - f_{ep_\omega} - f_{hp_\omega}), \qquad (1)$$

*Electronic address: ftvasko@yahoo.com

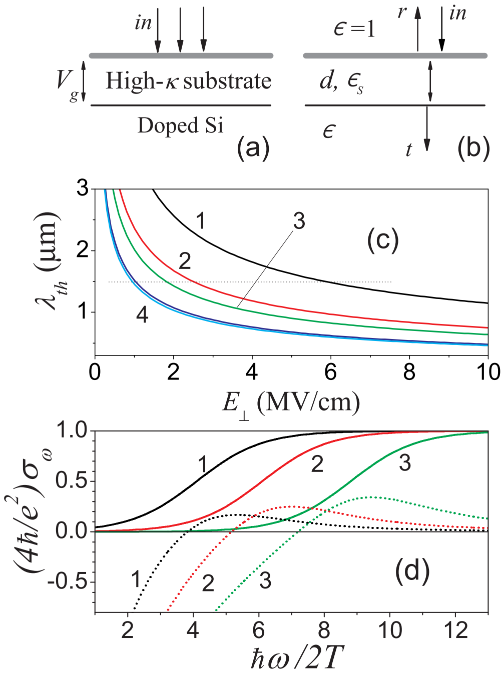

FIG. 1: (Color online) (a) Schematic view of graphene - high-κ substrate - heavily doped Si structure (V_g is gate voltage). (b) Normal propagation of incident (in), reflected (r), and transmitted (t) radiation through the graphene placed over substrate of thickness d on doped Si (ϵ_s and ϵ are the correspondent dielectric permittivities). (b) Threshold wavelenthes λ_{th} versus transverse field $E_\perp$ for structures with different substrates: SiO_2 (1), AlN (2), Al_2O_3 (3), and HfO_2 (4) (the results for ZrO_2 are similar to curve (4)). Dashed line is correspondent to the telecommunication wavelength, 1.55 μm. (c) Spectral dependences of $\mathrm{Re}\sigma_\omega$ and $\mathrm{Im}\sigma_\omega$ (solid and dotted curves) at room temperature for concentrations: 10^{12} cm^{-2} (1), 2×10^{12} cm^{-2} (2), 4×10^{12} cm^{-2} (3).

$$\mathrm{Im}\sigma_\omega \simeq \bar{\sigma}_\omega - \frac{e^2}{4\hbar p_\omega}\mathcal{P}\int\limits_0^\infty \frac{dpp^2}{p_\omega^2-p^2}\left(f_{ep}+f_{hp}\right).$$

In a doped graphene, when $E_\perp$ is strong enough, the Pauli blocking factor in $\mathrm{Re}\sigma_\omega$ is written through electron and hole distribution functions, $f_{e,h\ p}$, taken at $p_\omega = \hbar\omega/(2v)$, where $v = 10^8$ cm/s is the velocity of quasiparticles. Mention, that in the absence of carriers $\mathrm{Re}\sigma_\omega$ does not depend on any material parameters. [11] In the imaginary part of σ_ω we eliminate the contribution of the non-doped graphene $\bar{\sigma}_\omega$, see Refs. 12 and 13, and the carriers contribution is connected with $\mathrm{Re}\sigma_\omega$ through the Kramers-Kronig relation, where $\mathcal{P}$ means the principal value of integral. The response of N-layer epitaxial graphene [14] is described by the total conductivity $N\sigma_\omega$.

We restrict ourselvers to the geometry of normal propagation of the incident (in-), reflected (r-), and transient (t-) waves through the structure "N-layer graphene - dielectric substrate - doped Si", as it is shown in Fig. 1a. The in-plane electric field $E(z)\exp(-i\omega t)$ is governed by the wave equation: [1, 13]

$$\frac{d^2E(z)}{dz^2} + \epsilon_\omega(z)\left(\frac{\omega}{c}\right)^2 E(z) = 0, \tag{2}$$

where $z \neq 0$ and the permittivity $\varepsilon_\omega(z)$ is equal to the constant ε_s in the substrate layer with the thickness d (at $0 < z < d$), while in the thick Si the dispersion ε_ω should be taken into account, see Ref. 15. The boundary conditions at N-layer graphene sheet, where $z \to 0$, takes the form

$$\left.\frac{dE(z)}{dz}\right|_{-0}^{+0} + i\frac{4\pi\omega}{c^2}N\sigma_\omega E(z=0) = 0, \qquad E(z)|_{-0}^{+0} = 0. \tag{3}$$

These expressions contain the contribution of surface current, proportional to $N\sigma_\omega$, that determines the jump of $[dE(z)/dz]$, while $E(z)$ is continuous. At the substrate-Si interface we use the two conditions of continuity:

$$\left.\frac{dE(z)}{dz}\right|_{d-0}^{d+0} = 0, \qquad E(z)|_{d-0}^{d+0} = 0. \tag{4}$$

Outside of the graphene sheet the solution of electrodynamic problem (2)-(4) should be written in the form

$$E(z) = \left\{\begin{array}{cc} E_{in}e^{ik_\omega z} + E_r e^{-ik_\omega z} & z<0 \\ E_+ e^{i\tilde{k}_\omega z} + E_- e^{-i\tilde{k}_\omega z} & 0<z<d \\ E_t e^{i\bar{k}_\omega z} & d<z \end{array}\right. . \tag{5}$$

Here the amlitudes for in- and r-waves ($z<0$), t-wave ($z>d$), and for the field $E_\pm$ in the dielectric substrate (at $0<z<d$) are introduced. In Eq.(5) the wave vectors $k_\omega = \omega/c$ (to the left), $\tilde{k}_\omega = \sqrt{\epsilon_s}\omega/c$ (to the right), and $\bar{k}_\omega = \sqrt{\epsilon_\omega}\omega/c$ (in the dielectric substrate) are introduced as well. Using the boundary conditions (3) and (4) we get the system of linear equations for the amlitudes above. The solution of such a system determines the transition and reflection coefficients, T_ω and R_ω, according to

$$T_\omega = \sqrt{\epsilon_\omega}\frac{|E_t|^2}{E_{in}^2}, \qquad R_\omega = \frac{|E_r|^2}{E_{in}^2}. \tag{6}$$

According to energy conservation law, which connects T_ω and R_ω with the relative absorption coefficient ξ_ω, one obtains:

$$T_\omega + R_\omega + \xi_\omega = 1. \tag{7}$$

As a result, variations of T_ω and R_ω are correlated due to the Pauli blocking effect which leads to a jump of ξ_ω.

The direct expressions for the transmission and reflection coefficients take form

$$T_\omega = \frac{4\sqrt{\epsilon_\omega}}{|A_\omega^{(+)}|^2}, \qquad R_\omega = \left|\frac{A_\omega^{(-)}}{A_\omega^{(+)}}\right|^2. \tag{8}$$

where $A_\omega^{(\pm)}$ are expressed through the dynamic conductivity and the structure parameters according to

$$A_\omega^{(\pm)} = \sqrt{\epsilon}\cos\tilde{k}_\omega d - i\sqrt{\epsilon_s}\sin\tilde{k}_\omega d \tag{9}$$
$$+\left(\frac{4\pi\sigma_\omega}{c}\pm1\right)\left(\cos\tilde{k}_\omega d - i\sqrt{\varepsilon/\varepsilon_s}\sin\tilde{k}_\omega d\right).$$

In the case $\epsilon_\omega = \epsilon_s$ the oscillating factors eliminate from (9), and Eqs. (8) are in agreement with the previous results. [1, 13] Taking into consideration the interference on the substrate, when $\epsilon_\omega \neq \epsilon_s$, the spectral dependences of T_ω and R_ω are determined by carriers concentration (through variations of $E_\perp$ or V_g), the dielectric substrate thickness d, and the permittivities ε_s and ε_ω. We have neglected a weak absorption in Si and used ε_s for SiO_2 and high-κ dielectrics from Refs. 15 and 16, respectively.

III. RESULTS

Performing the numerical integration in Eq. (1) and using Eqs. (8, 9) one obtains the transmission and reflection coefficients. Below we analyze the dependences of T_ω and R_ω on the applied field $E_\perp$, which determines the carriers concentration, for the substrates of various thickness on the base of high-κ dielectrics or SiO_2. The computations were performed for near-IR and mid-IR spectral regions (λ =1.55 μm and 10.6 μm).

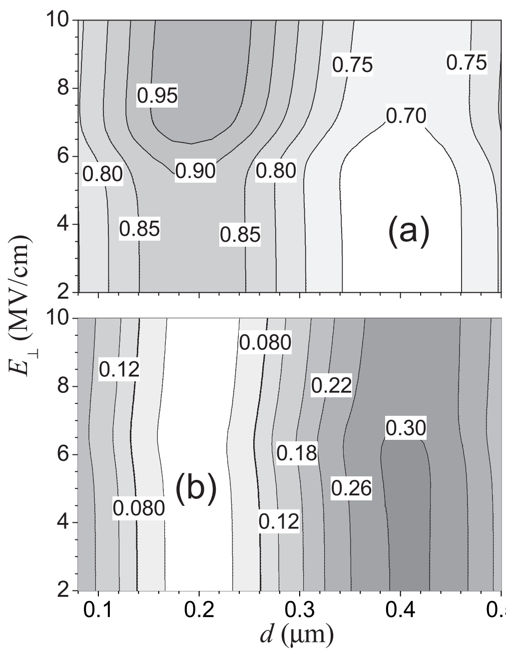

FIG. 2: (Color online) (a) Contour plot of transmission coefficient of graphene over Al_2O_3 substrate as a function of applied field $E_\perp$ and thickness d. (b) The same for reflection coefficient.

A. High-κ substrates

We examine first the modulation of the telecommunication range radiation, λ =1.55 μm, by the structures of 5-layer graphene on high-κ substrate at room temperature. Figures 2(a) and 2(b) show the contour plots of T and R versus $E_\perp$ and d for the case of Al_2O_3 substrate. One can see, that the change of T versus $E_\perp$ is ∼10% near the transmission maximum, and the modification of T by interference can be as large as 0.3 if d is in the range 0.1 - 0.5 μm. Similarly, the change of R versus $E_\perp$ does not exceed several %, while the modification of R versus d can be of 0.3 order. The maximum of T corresponds the minimum of R and vise versa.

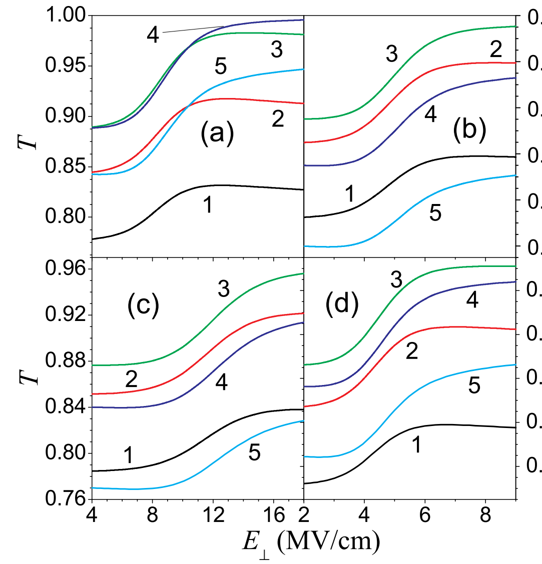

FIG. 3: (Color online) Transmissivity T at wavelength 1.55 μm versus $E_\perp$ for different substrates: (a) Al_2O_3, (b) HfO_2, (c) AlN, and (d) ZrO_2. Curves 1 - 5 are correspondent to the thicknesses d =0.08, 0.12, 0.16, 0.2, and 0.24 μm.

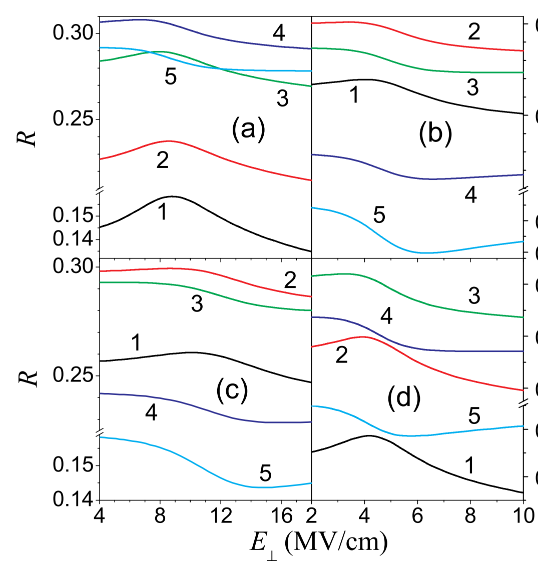

FIG. 4: (Color online) Reflectivity R at wavelength 1.55 μm versus $E_\perp$ for the same substrates as in Fig. 3(a-d). Curves 1 - 5 are correspondent to the thicknesses d =0.28, 0.32, 0.36, 0.4 and 0.44 μm.

Gate-voltage-induced modification of transmission is presented in Fig. 3 for different high-κ substrates at sev-

eral thicknesses near the maximum of T. Similar dependences for R are presented in Fig. 4 near the reflection maximum, corresponding to the greater thicknesses. Besides the essential dependence on thickness, T and R depend also on high-frequency and static permittivity of the materials under consideration. Therefore, the effective modulation for Al_2O_3 and AlN occurs in the range $E_\perp \sim 8$ - 12 MV/cm, and for HfO_2 and ZrO_2 the weaker fields $E_\perp \sim 4$ - 6 MV/cm are needed. The modulation depth for transmission exceeds in several times the modulation depth for reflection. The effective modulation interval, corresponding the region of the jump in absorption, becomes narrower with the decrease of temperature.

B. SiO_2 substrate

Now we are going to examine the structures "graphene - SiO_2 - Si", where the permittivities are smaller. Therefore the effective modulation for transmission of near-IR radiation takes place at $E_\perp \sim 25$ - 35 MV/cm, see Fig. 5(a), i.e. it needs stronger fields than the threshold of single-layer graphene on SiO_2 substrate ~ 6 MV/cm, see Fig. 1(b). The modulation of R in the same range of fields does not exceed several percents, see Fig. 5(b). It should be noted, that these fields $E_\perp$ are of the same order of values, as a breakdown field, therefore a possibility of modulation in this case needs a special verification.

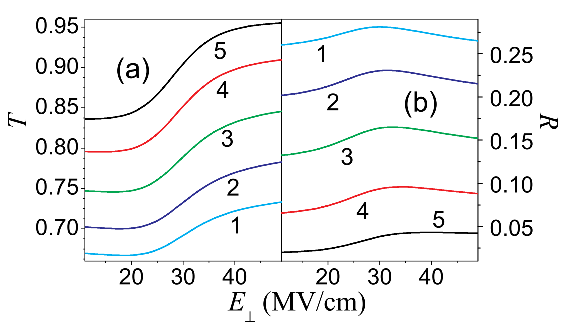

FIG. 5: (Color online) Transmissivity (a) and reflectivity (b), T and R, at wavelength 1.55 μm versus $E_\perp$ for SiO_2 substrate. Curves 1 - 5 are correspondent to the thicknesses d =0.24, 0.28, 0.32, 0.36 and 0.4 μm.

The effective modulation of transmission (over 5%, see Fig. 6(a)) takes place in mid-IR spectral region, for λ =10.6 μm. The applied field in this case does not exceed 2 MV/cm, but the substrate thickness should be greater because of the increase of λ. The corresponding modulation of reflection does not exceed several percents as well, see Fig. 6(b).

For the single layer graphene the modulation depth obviously can not be greater, than 2.3%. However, this modulation of transmission occurs for much lower fields, than in the previous cases under examination, 200 kV/cm, and the jump region becomes rather narrow with the decrease of temperature, see Figs. 7a, b.

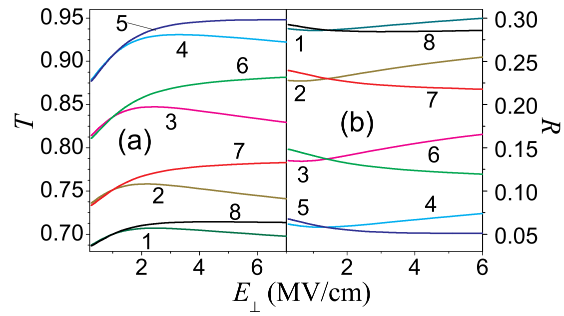

FIG. 6: (Color online) Transmissivity (a) and reflectivity (b) versus $E_\perp$ for five-layer graphene over SiO_2 substrate at wavelength 10.6 μm and room temperature. Curves 1 - 8 are correspondent to the thicknesses d =0.3, 0.6, 0.9, 1.2, 1.5, 1.8, 2.1 and 2.4 μm.

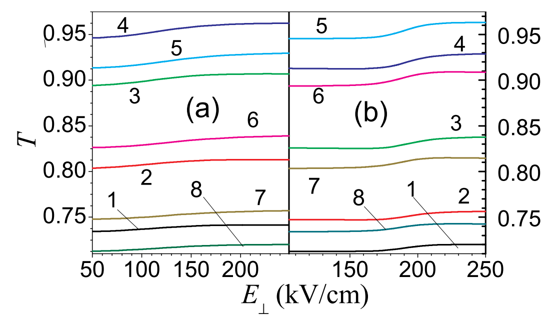

FIG. 7: (Color online) Transmissivity at wavelength 10.6 μm versus $E_\perp$ for a sigle layer graphene over SiO_2 substrate at temperatures 77 K (a) and 20 K (b). Curves 1 - 8 are correspondent to the same thicknesses as in Fig. 6.

IV. CONCLUDING REMARKS

The results obtained clearly demonstrate the possibility for realization of the modulator for telecommunication spectral range ($\sim$1.5 μm) on the base of multilayer graphene, placed over high-κ substrate. The effective modulation can be realized in this case for the applied fields $\sim$5 MV/cm, while for the case of SiO_2 substrate the field should be $\sim$20 MV/cm comparable to a breakdown value. The modulation depth for multi-layer (N =5-10) graphene can be as large as 10-20% ($\sim$2% per one layer). The same efficiency of modulation for the mid-IR radiation ($\sim$10.6 μm) can be realized for the applied fields not stronger than 2 MV/cm for the low temperature region.

The consideration performed takes into account the contribution of interband transitions, described by the complex dynamic conductivity, and the radiation interference on the structure "vacuum - graphene - substrate - doped Si" for the case of normal propagation of radiation. The modulation is determined by the Pauli blocking effect under the change of the carriers concentration by the gate voltage, therefore the time of modulation is governed by the recombination time of the excess concentration of carriers, or by the time of injection from contacts.

Next, we discuss the assumptions used in our calcu-

lations, which are rather standart ones. The dynamic conductivity of the carriers in the spectral region under examination is described properly with the use of the linear dispersion law of carriers in graphene. The phenomenological description of the dispersion of $Im\sigma_\omega$ due to the transitions from the valence band (see Refs. 12 and 13) does not change the results essentially due to the smallness of its contribution for the spectral range under consideration. The study of the declined propagation of radiation is more complicated, and the modulation efficiency in this case decreases. Moreover, the modulation efficiency can also be reduced in mid-IR range due to the absorption of radiation in the doped Si. It should be noted, that modulation of electron concentration in the gate gives a weak contribution to IR response and can be neglected in comparison to the Pauli blocking effect in graphene.

In conclusion, the results obtained should stimulate the experimental study of the electrooptical modulation of the near-IR radiation by the structure of multilayer graphene over high-κ dielectric substrate at room temperature and high gate voltages (concentrations). For the mid-IR spectral region the effective modulation can be realized at low temperatures.

Acknowledgments

This work was supported by the State Fundamental Research Fund of Ukraine (Grant 40.2/069).

[1] M. Orlita and M. Potemski, Semicond. Sci. Technol. **25** 063001 (2010); F. Bonaccorso, Z. Sun, T. Hasan and A. C. Ferrari, Nature Photonics **4**, 611 (2010); L.A. Falkovsky, Phys. Usp. **51**, 887 (2008).
[2] P. Blake, K. S. Novoselov, A. H. Castro Neto, D. Jiang, R. Yang, T. J. Booth, A. K. Geim, and E. W. Hill, Appl. Phys. Lett. **91**, 063124 (2007); D. S. L. Abergel, A. Russell, and V. I. Falko, Appl. Phys. Lett. **91**, 063125 (2007).
[3] Z. Sun, D. Popa, T. Hasan, F. Torrisi, F. Wang, E. J. R. Kelleher, J. C. Travers, V. Nicolosi, and A. C. Ferrari, Nano Res. **3**, 653 (2010); F.T. Vasko, Phys. Rev. B **82**, 245422 (2010).
[4] Z. Q. Li, E. A. Henriksen, Z. Jiang, Z. Hao, M. C. Martin, P. Kim, H. L. Stormer, and D. N. Basov, Nature Physics **4**, 532 (2008).
[5] F. Wang, Y. Zhang, C. Tian, C. Girit, A. Zettl, M. Crommie, and Y. R. Shen, Science **320**, 206 (2008).
[6] M. Liu, X. Yin, E. Ulin-Avila, B. Geng, T. Zentgraf, L. Ju, F. Wang, and X. Zhang, Nature, **474**, 64 (2011).
[7] Q. Bao, H. Zhang, B. Wang, Z. Ni, C. H. Y. X. Lim, Y. Wang, D. Y. Tang, and K. P. Loh, Nature Photonics **5**, 411 (2011).
[8] L. A. Falkovsky and S. S. Pershoguba, Phys. Rev. B **76**, 153410 (2007); L. A. Falkovsky, Phys. Usp. **51**, 887 (2008).
[9] M. Cardona, *Modulation Spectroscopy* (Academic Press, New York, 1969).
[10] F.T. Vasko and A.V. Kuznetsov, *Electron States and Optical Transitions in Semiconductor Heterostructures* (Springer, New York, 1998).
[11] T. Stauber, N. M. R. Peres, and A. K. Geim, Phys. Rev. B**78**, 085432 (2008).
[12] M. Bruna and S. Borini, Appl. Phys. Lett. **94** 031901 (2009).
[13] M. V. Strikha and F.T. Vasko, Phys. Rev. B **81**, 115413 (2010).
[14] W. A. de Heer, C. Berger, X. Wu, M. Sprinkle, Y. Hu, M. Ruan, J. A. Stroscio, P. N. First, R. Haddon, B. Piot, C. Faugeras, M. Potemski, J.-S. Moon, J. Phys. D: Appl. Phys. **43** 374007 (2010).
[15] C. M. Herzinger, B. Johs, W. A. McGahan, J. A. Woollam, and W. Paulson J. Appl. Phys. **83**, 3323 (1998).
[16] M. V. Fischetti, D. A. Neumayer, E. A. Cartier, J. Appl. Phys. **90**, 4587 (2001).